

COMPACT MICROSTRIP UWB BANDPASS FILTER WITH TRIPLE-NOTCHED BANDS

Junding Zhao¹, Jianpeng Wang^{1, *}, and Jia-Lin Li²

¹Ministerial Key Laboratory of JGMT, Nanjing University of Science and Technology (NUST), Nanjing 210094, China

²School of Physical Electronics, University of Electronic Science and Technology of China (UESTC), Chengdu 610054, China

Abstract—A new microstrip ultra-wideband (UWB) bandpass filter (BPF) with triple-notched bands is presented in this paper. The circuit topology and its corresponding electrical parameters of the initial microstrip UWB BPF are desired by a variation of genetic algorithm (VGA). Then, triple-notched bands inside the UWB passband are implemented by coupling a square ring short stub loaded resonator (SRSSLR) to the main transmission line of the initial microstrip UWB BPF. The triple-notched bands can be easily generated and set at any desired frequencies by varying the designed parameters of SRSSLR. For verification, a microstrip UWB BPF with triple-notched bands respectively centered at frequencies of 4.3 GHz, 5.8 GHz, and 8.1 GHz is designed and fabricated. Simulated and experimental results are in good agreement.

1. INTRODUCTION

In February 2002, the U.S. Federal Communications Commission allocated 3.1–10.6 GHz band as unlicensed spectrum for ultra-wideband (UWB) systems [1]. An UWB BPF, as one of the essential components of the UWB systems, has gained much attention in recent years. There are many techniques presented to design UWB bandpass filters. For example, multiple-mode resonator (MMR) [2, 3], multilayer coupled structure [4, 5], defected ground structure (DGS) [6], defected microstrip structure (DMS) [7], and the cascaded low-pass/high-pass filters [8] have been widely used to achieve UWB characteristics.

Received 31 May 2013, Accepted 7 September 2013, Scheduled 12 September 2013

* Corresponding author: Jianpeng Wang (eejpwang@gmail.com).

However, the existing wireless networks such as 3.5 GHz WiMAX signals, 5.8 GHz WLAN signals, and some 8.0 GHz satellite communication systems signals can easily interfere with UWB users, therefore, compact UWB BPF with multiple notched bands is emergently required to reject these interfering signals [9–15]. To achieve a notched band, one of the two arms in the coupled-line sections is extended and folded in [9]. On the other side, a coupling interdigital line is introduced to block undesired existing radio signals in [10]. However, these two methods can only achieve one notched band. Thus, to introduce dual notched bands, a coupled simplified composite right/left-handed resonator is introduced in [11], and two coupled stepped impedance resonators are employed in [12]. However, the selectivity designed with these two methods needs to be improved. By arranging two asymmetric meander open-loop resonators on middle layer and a C-shaped resonator on bottom layer [13] or embedding two open-circuit stubs into broadside-coupled stepped impedance resonators on middle layer [14], dual notched bands can be introduced into an UWB BPF. Additionally, by integrating short-circuited stub resonators [15] or embedding a quarter-wavelength coplanar waveguide resonators and inserting a meander slot-line in the detached-mode resonator [16] can also realize dual notched bands. However, these designs are based on multilayer technology which will increase fabrication cost. A new method based on wave's cancellation theory has been proposed to design an UWB BPF with dual notched band in [17]. However, the center frequencies and bandwidths of the notched bands cannot be adjusted. Two tri-section stepped impedance resonators and a parallel gap-coupled microstrip resonator are used in [18], and two L-shaped folded shunt open-circuited stubs are placed on the feed lines in [19] to achieve triple notched bands. However, the performance of the filters are not ideal. Furthermore, design efficiencies of the filters mentioned above need to be improved.

In this paper, we present a new UWB BPF with triple-notched bands. The initial microstrip UWB BPF is designed by a variation of genetic algorithm (VGA) to simultaneously search for the appropriate circuit topology and its corresponding electrical parameters. By improving the fitness evaluation, selection, crossover, and mutation, we overcome the two possible drawbacks of conventional GA, i.e., slow rate of convergence and local-best solution, thus to achieve better accuracy and high efficiency for UWB BPF design. Then, triple-notched bands property is achieved by coupling a square ring short stub loaded resonator (SRSSLR) to the main transmission line. The triple-notched bands can be easily generated and realized by controlling the locations of even-odd modes resonance frequency of the SRSSLR. The designed

methodology is very efficient and useful for filter synthesis though the design principle is simple. Moreover, the structure is compact, and the filter has good performance. Finally, the proposed filter is designed, fabricated, and measured. Good agreement between measured and simulated results is achieved.

2. UWB BANDPASS FILTER DESIGN

An arbitrary two-port microstrip circuit shown in Fig. 1(a) can be decomposed into basic circuit elements [20, 21] shown in Fig. 1(b). The circuit can be expressed as a data structure shown in Fig. 1(c). The data structure is composed of three parts. The first part coded in integer represents the topology of basic element. The second part coded in integer represents the way of connection to the previous element. The third part coded in floating number represents the corresponding electrical parameters. In the VGA, we define a basic circuit element as a gene and a set of basic circuit elements as a chromosome [22, 23]. Therefore, an arbitrary two-port circuit can be represented by a chromosome. Table 1 shows the details of the basic circuit elements. A special gene named *Empty* is introduced, which enables the representation scheme to describe a circuit with an

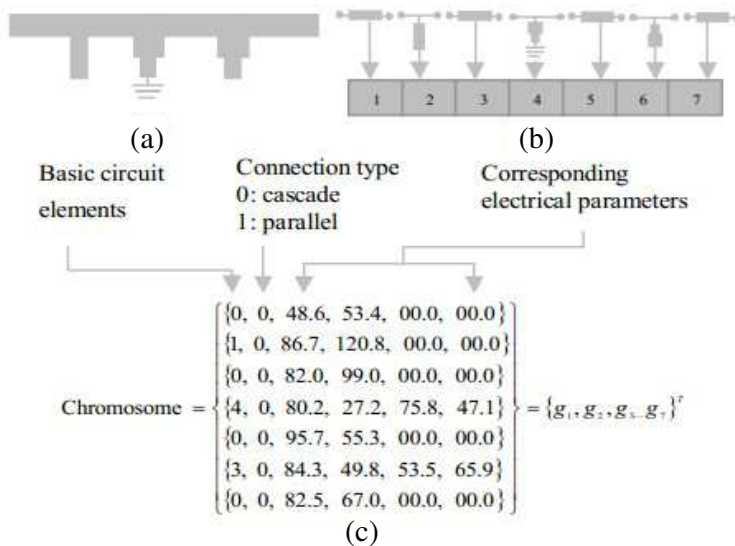


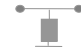





Figure 1. Representation scheme in the variation of genetic algorithm: (a) a typical microstrip circuit, (b) decomposition of the circuit in (a) into basic circuit elements, (c) chromosome of the circuit in (a).

Table 1. Details of the basic elements in the variation of genetic algorithm.

Category	Type	Name	Network Topology	Electrical Parameters
Basic Circuit Elements	0	TL		$Z_{01} \theta_{01}$
	1	Open		$Z_{01} \theta_{01}$
	2	Short		$Z_{01} \theta_{01}$
	3	SIR_Open		$Z_{01} \theta_{01} Z_{02} \theta_{02}$
	4	SIR_Short		$Z_{01} \theta_{01} Z_{02} \theta_{02}$
	5	Empty		0 0 0 0

arbitrary number of basic circuit elements and orders. In this work, we adopt a variation of genetic algorithm to design a microstrip UWB BPF with improved design efficiency.

2.1. Initialization

The initial population has an effect on the convergence, so we make every chromosome randomly initialize within the specific electrical parameters range of every basic element for better convergence in this scheme. Moreover, it is necessary to assign upper and lower limits according to various designs and engineering requirements. Due to the tolerance of the fabrication, the minimum width is limited to 0.1 mm, which corresponds to a microstrip line with a characteristic impedance of 137Ω . Meanwhile, to lower the junction discontinuity effects, the maximum line width is chosen to be 2 mm, which corresponds to a microstrip line with a characteristic impedance of 40Ω .

2.2. Fitness Evaluation

The transmission-line models are used to calculate scattering parameters (S_{21}) to effectively evaluate the frequency response of a chromosome. We make $ABCD$ matrix multiplication as cascade no matter the basic element is in series or parallel connection. It should be mentioned that the gene named *Empty* represents unit matrix. The method will improve the calculation speed of procedures and efficiency of the algorithm. The desired function is shown in Fig. 2, and the

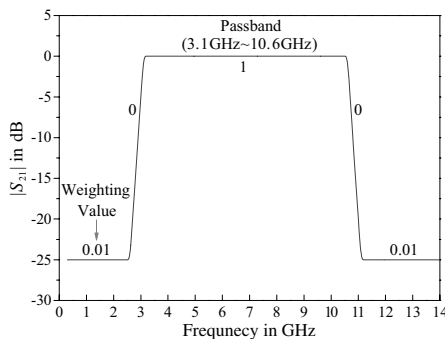


Figure 2. The desired function of the proposed initial UWB BPF.

fitness value is defined by:

$$F = \sum_{i=1}^N w_i f_i \tag{1}$$

where w_i represents the weighting value at the i th sampling point, f_i the square deviation between the calculated scattering parameter and the desired value at the i th sampling point, and N the number of sampling points.

2.3. Genetic Operator

Although the roulette wheel selection based on the proportionate selection is widely used in the GA, there is a drawback that the type of fitness function has an effect on the convergence. Thus, in this paper, the tournament selection is used.

Crossover operator is an important operator and plays a decisive role in global convergence of the algorithm. The way of the crossover decides whether we can find the optimal solution and the speed of finding the optimal solution. Therefore, the scheme employs a high efficiency crossover method of combining bubble sort with single-point crossover.

Mutation as a reproduction operator has a key role in getting out from the trap of the local optimum solution and keeping the diversity of population. In this work, mutation is carried out to randomly alter the values of genes in a parent chromosome with probability.

2.4. Result and Performance

Here, an initial microstrip UWB BPF is desired by a variation of genetic algorithm. The study is completed on a computer with a 2-GHz microprocessor, and the computing time of the example is only

1.8 min. For the design, the best chromosome after 18 generations consists of four Empty elements, five transmission lines, and four stubs. The proposed filter is realized on the substrate Duroid 5880 ($\epsilon_r = 3.38$, $h = 0.508$, $\tan \delta = 0.0027$). Table 2 lists the electrical and final physical parameters. It should be mentioned that the values in Table 2 are calculated by the following steps: Firstly, we transform the chain of $ABCD$ matrix for the chromosome to the scattering matrix. Secondly, we search for the optimal solution by optimizing the topology and its corresponding electrical parameters according to the design specification shown in Fig. 2. Thirdly, we convert the achieved electrical parameters to original physical parameters according to the corresponding relationship. Finally, we construct the filter model in HFSS, i.e., the proposed initial UWB BPF layout in Fig. 3, according to the original physical parameters. Notice that we have slightly adjusted some initial physical parameters considering the discontinuity effects and fringing capacitances. The simulated scattering parameters are shown in Fig. 3. Referring to Fig. 3, the proposed UWB BPF has an insertion loss better than 3 dB over the 3.44–11.55 GHz bandwidth, and the upper-stopband with -10 dB attenuation is up to 15 GHz. In addition, the return loss is under -20 dB over most part of the passband.

Table 2. Electrical and physical parameters of the initial UWB BPF.

No.	Name	Electrical Parameters (at $f_0 = 6.9$ GHz)							
		Physical Parameters in mm							
		z_{01}	θ_{01}	z_{02}	θ_{02}	W_{01}	L_{01}	W_{02}	L_{02}
1	Short	97.8	70.3	0	0	0.3	5.4	0	0
2	TL	52.2	47.8	0	0	1.1	3.5	0	0
3	Empty	0	0	0	0	0	0	0	0
4	TL	72.7	66.7	0	0	0.6	5	0	0
5	TL	67.3	71.0	0	0	0.7	5.3	0	0
6	Empty	0	0	0	0	0	0	0	0
7	SIR_Short	52.2	66.9	67.3	21.4	1.1	4.9	0.7	1.6
8	TL	58.6	74.3	0	0	0.9	5.5	0	0
9	Empty	0	0	0	0	0	0	0	0
10	Open	72.7	20.6	0	0	0.6	1.5	0	0
11	Empty	0	0	0	0	0	0	0	0
12	TL	72.9	37.3	0	0	0.6	2.8	0	0
13	SIR_Short	87.3	84.0	67.3	20.1	0.4	6.4	0.7	1.5

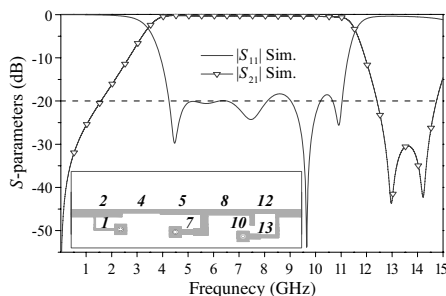


Figure 3. Simulated performance of proposed initial UWB BPF.

3. SQUARE RING SHORT STUB LOADED RESONATOR (SRSSLR) ANALYSIS

To realize band-notched characteristics, we introduce a square ring short stub loaded resonator (SRSSLR) into the initial UWB BPF. This structure is simple and flexible for blocking undesired narrow band radio signals that may appear in UWB band. The concept of the square ring loaded resonator (SRLR) has been extensively studied to develop various types of microwave devices [24]. It consists of two open folded microstrip lines and a square ring. Here, the proposed SRSSLR is composed of SRLR by a centrally loaded short-end stub. Fig. 4 shows the layout of a SRSSLR coupled to one main transmission line section.

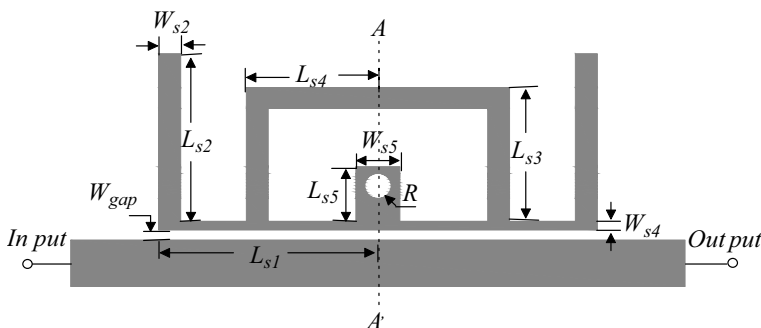


Figure 4. Layout of the coupled SRSSLR.

The resonance properties of SRSSLR can be analyzed based on even- and odd-mode method. Under mode excitation, the resonator electrical field distribution of the resonator exhibits either an even or an odd mode distribution property as shown in Fig. 5. For the odd mode, the electrical fields exhibit an anti-symmetric distribution along the $A-A'$ axis and there is no electrical field on the short-end stub as

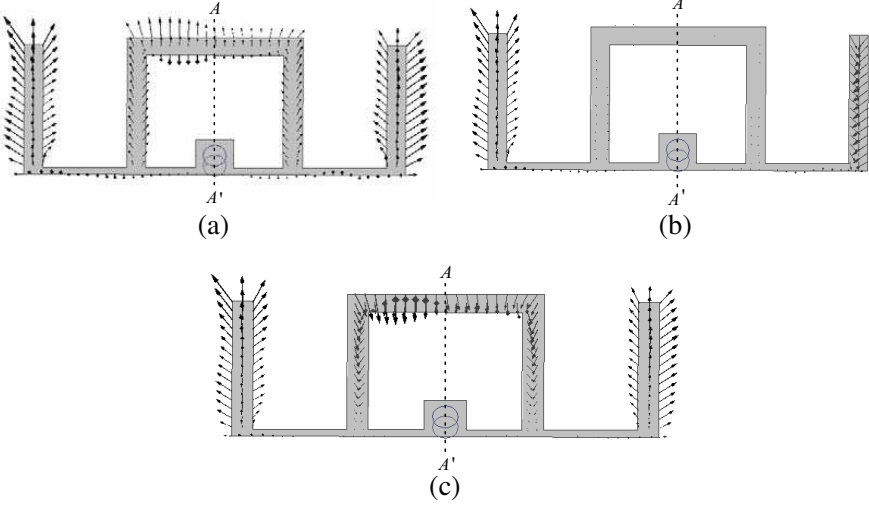


Figure 5. Electrical field distribution of the SRSSLR: (a) even mode, (b) odd mode, (c) even mode.

shown in Fig. 5(b). While for the even mode, the electrical fields exhibit a symmetric distribution along the $A-A'$ axis as shown in Figs. 5(a) and (c). Thus, based on the electrical field distribution property, the even-odd mode resonant frequency can be expressed as:

$$f_{notch} = \frac{c}{\lambda_{notch} \sqrt{\varepsilon_{eff}}} \quad (2)$$

$$f_{notch-even1} = \frac{c}{4(L_{S1} + L_{S2} + L_{S5}) \sqrt{\varepsilon_{eff}}} \quad (3)$$

$$f_{notch-odd1} = \frac{c}{4(L_{S1} + L_{S2}) \sqrt{\varepsilon_{eff}}} \quad (4)$$

$$f_{notch-even2} = \frac{c}{2(L_{S2} + L_{S3} + L_{S4}) \sqrt{\varepsilon_{eff}}} \quad (5)$$

where λ_{notch} is the wavelength of the center frequency of the notched band, f_{notch} the center frequency of the notched band, ε_{eff} the effective dielectric constant, and c the light speed in free space.

The frequency characteristics of the coupled SRSSLR with various dimensions are investigated by HFSS 11.0 to validate the multi-mode resonant property as shown in Fig. 6. It can be seen that the frequency locations of the triple notched bands move down simultaneously as increasing the dimensions of L_{s2} . While only the first notched band increases as decreasing L_{s5} . As for the frequency location of third notched band, it will move up as decreasing L_{s3} . Thus, by

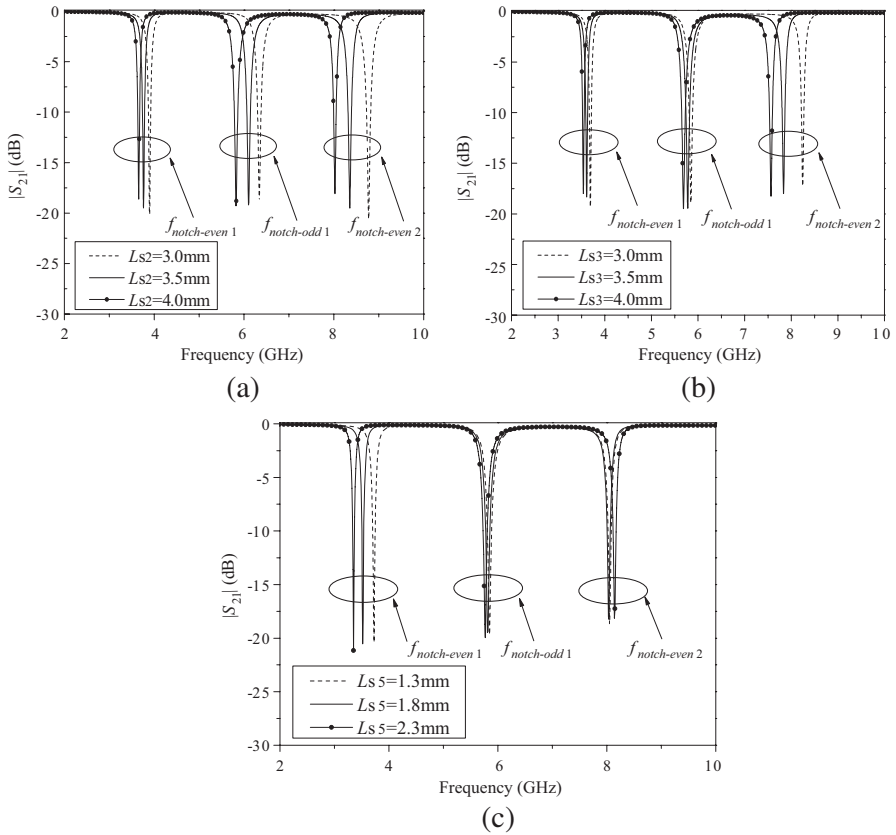


Figure 6. Simulated S -parameters of the coupled SRSSLR with various dimensions: (a) L_{S2} , (b) L_{S3} , (c) L_{S5} .

appropriately varying the resonator dimensions, triple notched bands can be achieved at desired frequencies.

The bandwidth of the notched band can be controlled by tuning the coupling coefficient k_m of the coupled SRSSLR as illustrated in Fig. 7. It should be mentioned that the coupling coefficient k_m is defined by:

$$k_m = \frac{f_{notch-odd1}^2 - f_{notch-even1}^2}{f_{notch-odd1}^2 + f_{notch-even1}^2} \quad (6)$$

Referring to Fig. 7(a), the coupling coefficient k_m decreases as W_{gap} increases. Referring to Fig. 7(b), the stronger coupling between the SRSSLR and main transmission line is, the wider bandwidth of the notched band will appear. Thus, the bandwidth of the notched band can be controlled by suitably shifting the coupling coefficient between

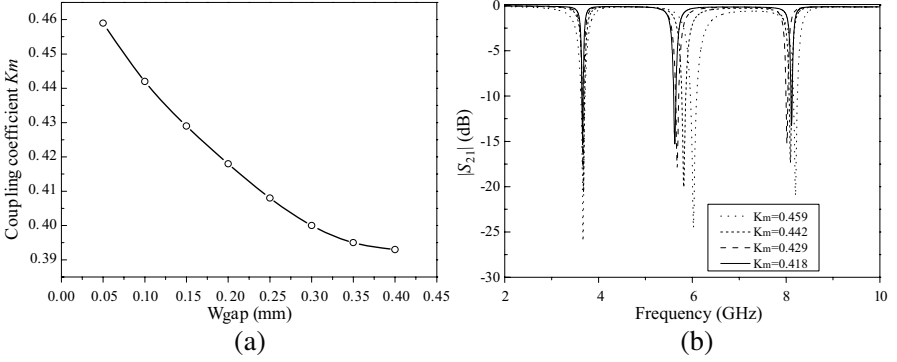


Figure 7. (a) Simulated coupling coefficient k_m of the coupled SRSSLR with different W_{gap} , (b) relationship between notched bands performance and different coupling coefficient k_m .

the SRSSLR and the main transmission line.

In this paper, the coupling coefficient is selected as $k_m = 0.442$ and the SRSSLR dimensions are as follows: $W_{s2} = 0.5$ mm, $W_{s4} = 0.5$ mm, $W_{s5} = 1.0$ mm, $L_{s1} = 3.8$ mm, $L_{s2} = 3.7$ mm, $L_{s3} = 3.6$ mm, $L_{s4} = 2.5$ mm, $L_{s5} = 0.8$ mm, $W_{gap} = 0.1$ mm, $R = 0.3$ mm. Therefore, the final UWB BPF shown in Fig. 9 is realized by combining the SRSSLR with the initial UWB BPF designed in Section 2.

4. EXPERIMENTAL RESULTS

The designed UWB BPF is measured with an Agilent N5244A vector network analyzer. Fig. 8 shows the comparison between the simulated and measured results. It can be seen that the fabricated UWB BPF has

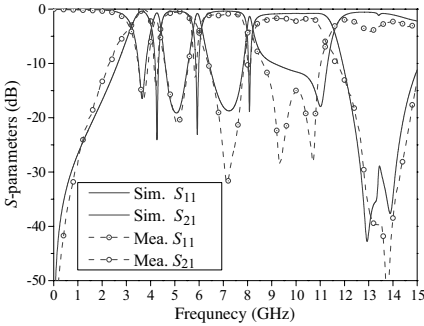


Figure 8. Simulated and measured S -parameters of the designed UWB BPF.

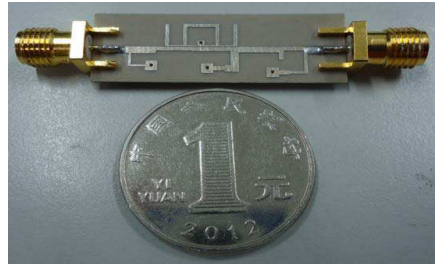


Figure 9. Photograph of the fabricated UWB BPF with triple-notched bands.

a pass-band from 3.1–10.9 GHz as we expected. Three notched bands with respective 3dB FBWs of 7.1%, 6.8%, and 4.9% are achieved, which ensure a high selectivity for the designed UWB filter. Inside each notched band, the attenuation is better than -15 dB at the center frequencies of 4.3, 5.8, and 8.1 GHz. The minor discrepancy between simulation and measurement results are mainly due to the

Table 3. Comparisons with other proposed UWB BPF with notched bands.

Ref.	Circuit size (λ_g : at 6.85 GHz)	Circuit dimension	Pass band (GHz)
[9]	0.81×0.17	2-D	3.6 ~ 10.2
[10]	0.81×0.10	2-D	3.1 ~ 10.6
[11]	1.16×0.68	2-D	2.8 ~ 10.9
[12]	0.98×0.63	2-D	3.1 ~ 11.0
[13]	0.53×0.51	3-D	2.6 ~ 9.6
[14]	1.18×0.26	3-D	3.2 ~ 10.3
[15]	0.36×0.46	3-D	2.8 ~ 10
[16]	0.95×0.7	3-D	4.5 ~ 10.7
[17]	0.88×0.19	2-D	3.2 ~ 12.0
[18]	1.27×0.28	2-D	3.2 ~ 12.4
[19]	2.29×0.69	2-D	2.5 ~ 10.6
Our work	1.03×0.38	2-D	3.1 ~ 10.9
Ref.	Insertion loss (dB)	Notch frequency (GHz) /attenuation (dB)	Upper stop-band (GHz)
[9]	0.6	5.59 > 15	26
[10]	1.0	5.75 > 20	12
[11]	1.0	5.85/8.05 > 15	14
[12]	1.0	5.2/5.8 > 15	12
[13]	1.5	3.5/5.8 > 15	11
[14]	1.0	5.38/6.0 > 10	18
[15]	0.6	5.23/5.81 > 20	15
[16]	1.5	5.47/6.05 > 20	18
[17]	1.0	6.55/8.62 > 20 > 20	15
[18]	1.2	5.63/6.47/8.93	16
[19]	2.0	5.57/6.49/9.05 > 15	12
Our work	0.8	4.3/5.8/8.1 > 15	15

reflections from the SMA connectors and the finite substrate. Fig. 9 shows the photograph of the fabricated UWB BPF. Comparisons with other reported UWB BPFs with notched bands are listed in Table 3. It shows that the proposed filter has good performance.

5. CONCLUSION

A new microstrip UWB BPF with triple highly rejected notched bands has been proposed and designed in this paper. The initial UWB BPF is efficiently designed by a variation of genetic algorithm. Then, triple-notched bands performance is easily generated and realized by controlling the resonance properties of the square ring short stub loaded resonator (SRSSLR). Good agreement between simulation and measurement results validates the introduced design method. The proposed filter is very useful for modern UWB wireless communication systems due to its distinct properties of simple topology, compact size, and good performance.

ACKNOWLEDGMENT

This work was supported by the National Natural Science Foundation of China under Grants No. 61101047, 61271025, the Zijin Foundation under Grant AB41372, and the Specialized Research Fund for the Doctoral Program by the Ministry of Education of China under Grant No. 20113219120015.

REFERENCES

1. FCC, "Revision of part 15 of the commission's rules regarding ultra-wide-band transmission system," 98–153, Tech. Rep., ET-Docket, 2002.
2. Zhu, L., S. Sun, and W. Menzel, "Ultra-wideband (UWB) bandpass filters using multiple-mode resonator," *IEEE Microw. Wireless Compon. Lett.*, Vol. 15, No. 11, 796–798, 2005.
3. Qiang, L., Y.-J. Zhao, Q. Sun, W. Zhao, and B. Liu, "A compact UWB HMSIW bandpass filter based on complementary split-ring resonators," *Progress In Electromagnetics Research C*, Vol. 11, 237–243, 2009.
4. Packiaraj, D., K. J. Vinoy, and A. T. Kalghatgi, "Analysis and design of two layered ultra wide band filter," *Journal of Electromagnetic Waves and Applications*, Vol. 23, Nos. 8–9, 1235–1243, 2009.

5. Wang, H., L. Zhu, and W. Menzel, "Ultra-wideband bandpass filter with hybrid microstrip/CPW structure," *IEEE Microw. Wireless Compon. Lett.*, Vol. 15, No. 12, 844–846, 2005.
6. Shobeyri, M. and M. H. Vadjed-Samiei, "Compact ultra-wideband bandpass filter with defected ground structure," *Progress In Electromagnetics Research Letters*, Vol. 4, 25–31, 2008.
7. Naghshvarian-Jahromi, M. and M. Tayarani, "Miniature planar UWB bandpass filters with circular slots in ground," *Progress In Electromagnetics Research Letters*, Vol. 3, 87–93, 2008.
8. Comez-Garcia, R. and J. I. Alonso, "Systematic method for the exact synthesis of ultra-wideband filtering responses using high-pass and low-pass sections," *IEEE Trans. on Microw. Theory and Tech.*, Vol. 54, No. 10, 3751–3764, 2006.
9. Wong, S. W. and L. Zhu, "Implementation of compact UWB bandpass filter with a notch-band," *IEEE Microw. Wireless Compon. Lett.*, Vol. 18, No. 1, 10–12, 2008.
10. Wei, F., L. Chen, X.-W. Shi, X. H. Wang, and Q. Huang, "Compact UWB bandpass filter with notched band," *Progress In Electromagnetics Research C*, Vol. 4, 121–128, 2008.
11. Wei, F., Q. Y. Wu, X. W. Shi, and L. Chen, "Compact UWB bandpass filter with dual notched bands based on SCRLH resonator," *IEEE Microw. Wireless Compon. Lett.*, Vol. 21, No. 1, 28–30, 2011.
12. Wu, H.-W., M.-H. Weng, and C.-Y. Hung, "Ultra wideband bandpass filter with dual notch bands," *Proc. Asia-Pacific Microwave Conf.*, 33–36, Yokohama, Japan, 2010.
13. Hsiao, P.-Y. and R.-M. Weng, "Compact tri-layer ultra-wideband bandpass filter with dual notch bands," *Progress In Electromagnetics Research*, Vol. 106, 49–60, 2010.
14. Hao, Z.-C., J.-S. Hong, S. K. Alotaibi, J. P. Parry, and D. P. Hand, "Ultra-wideband bandpass filter with multiple notch-bands on multilayer liquid crystal polymer substrate," *IET Microw. Antennas Propag.*, Vol. 3, No. 5, 749–756, 2009.
15. Hao, Z.-C., J.-S. Hong, J. P. Parry, and D. P. Hand, "Ultra-wideband bandpass filter with multiple notch bands using nonuniform periodical slotted ground structure," *IEEE Trans. on Microw. Theory and Tech.*, Vol. 57, No. 12, 3080–3088, 2009.
16. Luo, X., J.-G. Ma, K. S. Yeo, and E.-P. Li, "Compact ultra-wideband (UWB) bandpass filter with ultra-narrow dual- and quad-notched bands," *IEEE Trans. on Microw. Theory and Tech.*, Vol. 59, No. 6, 1509–1519, 2011.

17. Nosrati, M. and M. Daneshmand, "Compact microstrip UWB double/single notch-band BPF based on wave's cancellation theory," *IET Microw. Antennas Propag.*, Vol. 6, No. 8, 862–868, 2012.
18. Nosrati, M. and M. Daneshmand, "Developing single-layer ultra-wideband band-pass filter with multiple (triple and quadruple) notches," *IET Microw. Antennas Propag.*, Vol. 7, No. 8, 612–620, 2013.
19. Dong, Y. L., C.-M. Sun, W.-Y. Fu, and W. Shao, "Ultra-wideband bandpass filters with triple and quad frequency notched bands," *Journal of Electromagnetic Waves and Applications*, Vol. 26, Nos. 11–12, 1624–1630, 2012.
20. Hsu, M.-H. and J.-F. Huang, "Annealing algorithm applied in optimum design of 2.4 GHz and 5.2 GHz dual-wideband microstrip line filters," *IEICE Trans. on Electronics*, Vol. E88C, No. 1, 47–56, 2005.
21. Tsai, L.-C. and C.-W. Hsue, "Dual-band bandpass filters using equal-length coupled-serial- shunted lines and Z -transforms technique," *IEEE Trans. on Microw. Theory and Tech.*, Vol. 52, No. 4, 1111–1117, 2004.
22. Nicholson, G.-L. and M.-J. Lancaster, "Coupling matrix synthesis of cross coupled microwave filters using a hybrid optimisation algorithm," *IET Trans. on Microw. Antennas Propag.*, Vol. 3, No. 6, 1111–1117, 2009.
23. Zhao, Y.-X., F. Chen, H. Chen, N. Li, Q. Shen, and L. Zhang, "The microstructure design optimization of negative index metamaterials using genetic algorithm," *Progress In Electromagnetics Research Letters*, Vol. 22, 95–108, 2011.
24. Chen, J.-Z., N. Wang, Y. He, and C.-H. Liang, "Fourth-order tri-band bandpass filter using square ring loaded resonators," *Electronics Letters*, Vol. 47, No. 15, 858–859, 2011.